

The Optimization of An Industrial Ammonium Jarosite Production Circuit

*Dr. Corby G. Anderson¹, Camille M. Fleuriault¹, Dr. Larry G. Twidwell²

¹Kroll Institute for Extractive Metallurgy

George S. Ansell Department of Metallurgical and Materials Engineering
Colorado School of Mines Illinois Street Golden, Colorado USA

²The Center for Advanced Mineral and Metallurgical Processing
Montana Tech West Park Street Butte, Montana USA

ABSTRACT: The selective precipitation of iron as ammonium jarosite is a well-established industrial technology in base metals hydrometallurgy. It is a key technology in minimizing iron tenors which would be disruptive to downstream processing. It also provides a more readily filterable iron solid to better facilitate materials handling. This paper elucidates the fundamentals behind industrial iron precipitation. Then, the details of the successful optimization of an industrial ammonium jarosite circuit are presented.

Keywords: Iron, jarosite, copper, nickel, ammonia, optimization

Date of Submission: 24-09-2017

Date of acceptance: 14-12-2017

I. HYDROMETALLURGICAL IRON REMOVAL FUNDAMENTALS

Iron is the fourth most abundant element in the Earth's crust (5% by weight) and is often found in complex ores such as sulphide-bearing formations. Iron represents an issue though during leaching, a technology which is widely used for the treatment of this type of ore:

- Iron has the particularity of forming hydroxides when leached under certain conditions. Iron hydroxides form a viscous gel, which is difficult to filter and traps valuable elements such as silver.
- Iron is solubilized along with other metals and interferes with the subsequent extraction steps.

As a result, purification of the pregnant leach solutions is required to achieve economical extraction of base metals. In the 1960s, metallurgists developed iron precipitation processes for solution purification (Habashi, 1999, Mohemius, 2016). Nowadays, precipitation of iron bearing species, such as goethite, hematite or jarosite, has become one of the most common methods used in the industry to purify leach liquors. To be suitable, the precipitate has to be readily filterable and thus must not be too fine of particle size. Precipitation can take place in autoclaves at medium to high temperatures, under an oxygen or air overpressure (Tourre, 1984, Fleuriault 2016, Fleuriault Anderson Shuey, 2016)).

None of the precipitates from the goethite and jarosite processes is suitable for direct commercialization. Further refining is needed. In the production of hematite, ferrite materials can be considered as marketable products if they are pure enough. Table 1 summarizes and compares the characteristics of the three industrial iron precipitation processes, as presently used in the zinc industry.

Fundamentals of Iron Hydroxysulphate Phase Formation during Iron Precipitation Processes

During sulphide leaching processes, such as pressure oxidation, iron forms ferrous sulphate, which is oxidized to ferric sulphate. Hydrolysis of ferric sulphate then forms an iron precipitate. At temperatures >185°C in an oxidative environment, several iron species can form, but most often, hematite is the desirable product. The conditions for hematite formation are stringent and sometimes difficult to control. It is likely that other iron solids (called iron hydroxysulphates) precipitate along with the hematite (Fleming, 2010).

Iron hydroxysulphates are unwanted constituents in the hematite residue for several reasons:

- Poorer settling and filtration properties
- Relatively unstable compounds which may represent an environmental risk if stockpiled
- Trapping of precious metal values in their crystal structure resulting in lower PGM recovery
- In the case of gold cyanidation circuits, a high concentration of iron hydroxysulphates in the autoclave residue means high lime consumption and difficulties maintaining pH values >10 during the cyanidation step. There is a slight risk of forming toxic HCN.

Several publications have shown that the total amount of free acid in solution determines which iron species preferentially forms (Cheng et al., 2004; Fleming, 2010; Tourre, 1984; Umetsu et al., 1977). Depending on the leaching conditions, the limiting acid concentration for the formation of one or the other iron species varies. Because hematite is preferred over iron hydroxysulphates in the final product, the acid concentration is closely monitored during autoclave processing.

Table 1 – Comparison of the goethite, jarosite and hematite processes as used in the zinc industry (Gupta et al., 1990; Gathje, 2006)

Parameter	Goethite	Jarosite	Hematite
Compound formed	FeO.OH	MFe ₃ [(SO ₄) ₂ (OH) ₆] with M=K, Na, NH ₄	Fe ₂ O ₃
Temperature (°C)	70-90	90-100	>185
pH	2-3.5	1.5	Up to 2% H ₂ SO ₄
Anion present	Any	SO ₄ ²⁻	SO ₄ ²⁻
Cation added	None	Na ⁺ , K ⁺ , NH ₄ ⁺	None
Cationic impurities	Medium	Low	Low
Anionic impurities	Medium	High Medium	
Filterability	Very good	Very good	Very good
Fe left in solution (g/L)	<0.05	1-5	3
Metal recovery %	Zn 96 % Cu 90 % Ag 85 %	Zn 96 % Cu 90 % Ag 60-65%	Zn 98.2 % Cu 98.2 % Ag 98.2 %
Residue composition wt.%	Fe 40-45 % Zn 5-10 % S 2.5-5 %	Fe 25-30 % Zn 4-6 % S 10-12 %	Fe 50-60 % Zn 0.5-1 % S 2-3%
Moisture wt.%	50	50	10
Amount produced/t concentrate	0.25	0.40	0.18
Zn loss in t/t slab	0.025	0.025	0.002

II. IRON HYDROXYSULPHATE PRECIPITATE CHARACTERIZATION

The nomenclature of iron hydroxysulphate species varies depending on the authors. These compounds can also be referred to as ferric hydroxysulphate, basic iron sulphate or iron hydroxyl sulphate. Early work by Posnjak and Merwin (1922) reported many ferric sulphate salts but many of them are not crystalline species. Basic ferric sulphate, or BFS, is metastable and often composed of mixtures. As a result, such precipitates are quite difficult to characterize and few data are available. Posnjak and Merwin identified three series of BFIS. However, at the time, the authors did not exclude the possibility that other hydrated species also exist. The three series were subdivided and organized by the ratio Fe₂O₃ to SO₃. The following Table 2 presents the BFS already identified at the time of this study.

Table 2 – BFS compounds classified by their Fe₂O₃:SO₃ ratio (Posnjak, 1922)

Fe ₂ O ₃ : SO ₃ ratio	Formula	Crystal	Color	Name
3:4	3Fe ₂ O ₃ .4SO ₃ .9H ₂ O	Rhombohedral	Light-deep yellow	Carphosiderite ¹
1:2	Fe ₂ O ₃ .2SO ₃ .H ₂ O	Orthorhombic	Orange-yellow	
	Fe ₂ O ₃ .2SO ₃ .5H ₂ O	Monoclinic	Light yellow	
	2Fe ₂ O ₃ .5SO ₃ .17H ₂ O	Orthorhombic	Light-bright yellow	Copiapite
	Fe ₂ O ₃ .2SO ₃ .7H ₂ O		Yellowish	Amarantite
	Fe ₂ O ₃ .2SO ₃ .8H ₂ O		Yellowish	Castanite
2:5	Fe ₂ O ₃ .2SO ₃ .10H ₂ O		Yellowish	Fibroferrite

¹Carphosiderite is a discredited mineral name and nowadays corresponds to hydronium jarosite.

In the late 1970s, the iron hydroxysulphate minerals were divided in two series (Rossman, 1976 and Scordari, 1981):

- Compounds with the general formula $\text{Fe}(\text{OH})\text{SO}_4 \cdot n\text{H}_2\text{O}$, with the following members: basic ferric sulphate $\text{Fe}(\text{OH})\text{SO}_4$, butlerite/parabutlerite (they are polymorphs) $\text{Fe}(\text{OH})\text{SO}_4 \cdot 2\text{H}_2\text{O}$ and fibroferrite: $\text{Fe}(\text{OH})\text{SO}_4 \cdot 5\text{H}_2\text{O}$. According to several publications, the non-hydrated member of the BFS series is synthetic and has been obtained only in the laboratory.
- Jarosites. The main jarosite species are presented later in this paper.

Lazaroff et al. (1982) also make the distinction between crystalline jarosites and amorphous ferric hydroxysulphates, but refer to this last category as BFS. In order to simplify the nomenclature and avoid any confusion within the next sections, we will distinguish BFS ($\text{Fe}(\text{OH})\text{SO}_4$ and its hydrated species) from the jarosite compounds. We will consider BFS and jarosite as iron hydroxysulphates. The following Table 3 presents the most common BFS encountered in high temperature systems, using the most recent nomenclature.

Table 3 – Selected hydroxysulphates and oxy-hydroxysulfates of iron (adapted from Bigham, 2000)

Name	Formula
Copiapite	$\text{Fe}^{\text{II}}\text{Fe}_4^{\text{III}}(\text{SO}_4)_6(\text{OH})_2 \cdot 2\text{H}_2\text{O}$
Fibroferrite	$\text{Fe}^{\text{III}}(\text{SO}_4)(\text{OH}) \cdot 5\text{H}_2\text{O}$
Amarantite	$\text{Fe}^{\text{III}}(\text{SO}_4)(\text{OH}) \cdot 3\text{H}_2\text{O}$
Butlerite	$\text{Fe}^{\text{III}}(\text{SO}_4)(\text{OH}) \cdot 2\text{H}_2\text{O}$
Basic Ferric Sulphate	$\text{Fe}^{\text{III}}(\text{SO}_4)(\text{OH})$
-	$\text{Fe}_4^{\text{III}}(\text{SO}_4)(\text{OH})_{10}$
Schwertmannite	$\text{Fe}_8^{\text{III}}\text{O}_8(\text{OH})_6(\text{SO}_4) \cdot n\text{H}_2\text{O}$

III. JAROSITE PRECIPITATE CHARACTERIZATION

Jarosites are compounds of the general formula: $\text{MFe}_3(\text{SO}_4)_2(\text{OH})_6$, where M can be H_3O^+ , Na, K, NH_4^+ , Pb, Ag, Tl, Hg, Rb (Tourre, 1984). Silver-jarosite and potassium-jarosite are the two most stable compounds of the family. Other extensive substitutions occur for Fe^{3+} , SO_4^{2-} , OH^- . As for BFS, not all jarosites are naturally occurring. Out of nine species synthesized, only seven occur as minerals. The first mineral to be identified was potassium jarosite, in Andalusia, Spain in 1852. Table 4 lists all known jarosite species.

Table 4. Chemical and mineral names of jarosites (Dutrizac, 2000).

Formula	Chemical Name	Mineral Name
$\text{H}_3\text{OFe}_3(\text{SO}_4)_2(\text{OH})_6$	Hydronium Jarosite	Hydronium Jarosite
$\text{NaFe}_3(\text{SO}_4)_2(\text{OH})_6$	Sodium Jarosite	Natrojarosite
$\text{KFe}_3(\text{SO}_4)_2(\text{OH})_6$	Potassium Jarosite	Jarosite
$\text{RbFe}_3(\text{SO}_4)_2(\text{OH})_6$	Rubidium Jarosite	None
$\text{AgFe}_3(\text{SO}_4)_2(\text{OH})_6$	Silver Jarosite	Argentojarosite
$\text{NH}_4\text{Fe}_3(\text{SO}_4)_2(\text{OH})_6$	Ammonium Jarosite	Ammoniojarosite
$\text{TlFe}_3(\text{SO}_4)_2(\text{OH})_6$	Thallium Jarosite	Dorallcharite
$\text{Pb}_{1/2}\text{Fe}_3(\text{SO}_4)_2(\text{OH})_6$	Lead Jarosite	Plumbojarosite
$\text{Hg}_{1/2}\text{Fe}_3(\text{SO}_4)_2(\text{OH})_6$	Mercury Jarosite	None

IV. IRON HYDROXYSULPHATES COMPARISON

A spectroscopic analysis of the products of ferric sulphate hydrolysis was performed in 1996, with emphasis made on the amorphous species, which are compared to jarosite (Burgina et al., 1996). While jarosite dissolves very slowly, BFS are reactive in water. This difference is explained by the atomic arrangement of each species: jarosites are trimers, and amorphous BFS are tetramers (Figure 1). According to Burgina and al., the reactivity of BFS is caused by the small separation between neighboring iron atoms, short Fe-O distance and strong hydrogen bonds (creating a large number of highly acid centers). This would promote the oxidation of H_2O in O_2 and thus explain BFS reactivity in water.

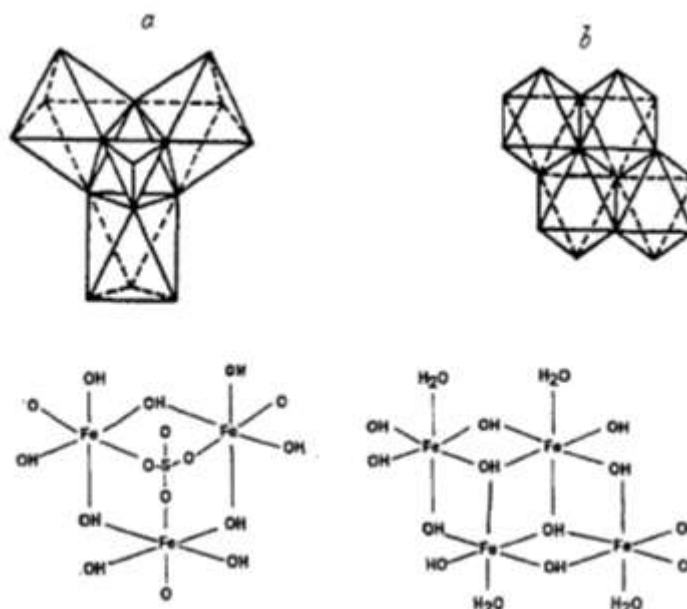


Figure 1 – Molecular structures of jarosite (trimer) and BFS (tetramer) (Burgina et al., 1996)

BFS are also reactive in the atmosphere (Posnjak et al., 1922), decomposing either to ferric hydroxide and gypsum (alkaline conditions) or ferric sulphate (acidic conditions). BFS can be formed by precipitation, hydrolysis or evaporation but none of these processes yielded a product that fully achieved equilibrium; thereby, mixtures were produced. In the case of pressure leaching, the main factors influencing BIS formation are acidity, temperature and iron concentration. BFS readily precipitate at high acidity (>20g/L) and lower temperatures (<200°C) (Fleming, 2010). As mentioned before, jarosite formation is favored by high acidity as well as well as the presence of some cations in relatively high concentrations (Na^+ , NH_4^+ , K^+ , Ag^+ or Pb^+). Additionally, BFS precipitation seems to be promoted by increasing ferric concentration. At 225°C, within the stability region of hematite, Dutrizac and Chen (2012) have observed that BFS becomes the predominant phase if the initial $[\text{Fe}^{3+}]$ concentration exceeds 22.3g/L (Dutrizac and Chen, 2012).Based on Posnjak and Merwin's work, Tourre (1984) produced a 3-D model of the hematite/sulphate system, as shown in Figures 2 and 3.

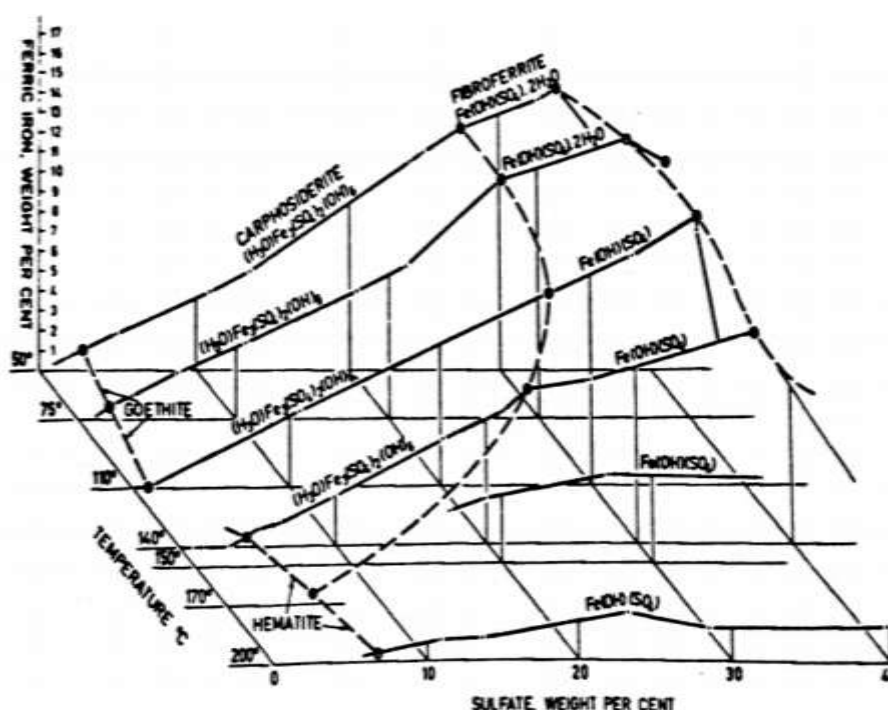


Figure 2 – The $\text{Fe}_2(\text{SO}_4)_3\text{-H}_2\text{SO}_4\text{-H}_2\text{O}$ system polytherm at 50 to 200°C and 0 to 40% SO_4 (Tourre, 1984)

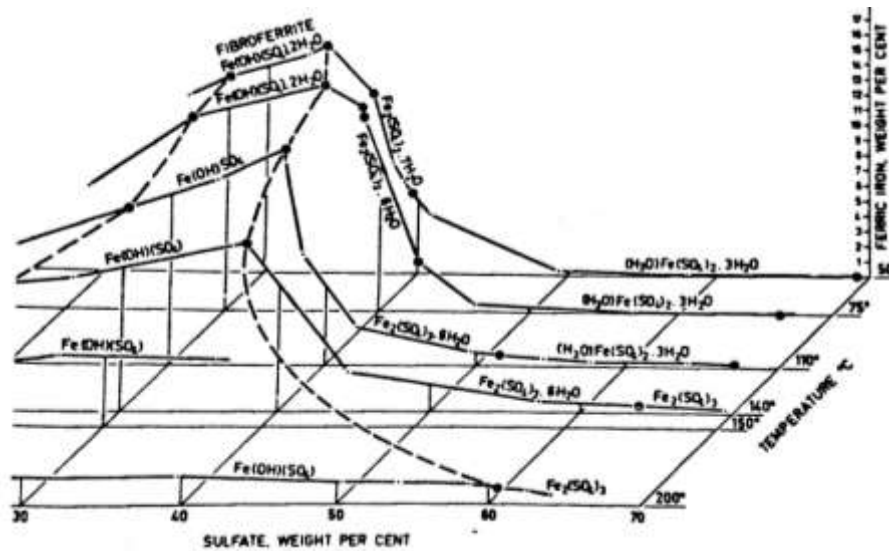


Figure 3 - The $Fe_2(SO_4)_3-H_2SO_4-H_2O$ system polytherm at 50 to 200°C and 30 to 70% SO_4 (Tourre, 1984)

These observations were confirmed in 1982 (Lazaroff et al., 1982). In the simple Fe-O-S system, hydronium jarosite has a limited area of stability, as it is one of the least stable jarosite species. If additional ions such as Na^+ , K^+ or NH_4^+ were present (which is extremely likely in a real industrial situation), jarosites would certainly replace BFS. In 1971, Babcan (1971) defined the area of stability of iron hydroxysulphates in the Fe-O-S system (see Figure 4). In more recent studies, BFS have been proven to be also stable at conditions which would normally lead to hematite formation (Dutrizac & Chen., 2012; Voigt et al., 1986). If the oxidation conditions were maintained for a longer time, the most stable phase would eventually form. As a result, from a thermodynamic point of view, iron hydroxysulphates are metastable.

Several hematite solubility studies have been conducted in order to identify the optimum conditions for iron oxide precipitation. At equilibrium and room temperature, Umetsu et al. (1977) proposed a linear relation between ferric concentration in g/L and free acidity:

$$\text{Log}[\text{Fe(III)}]_{\text{total}} = a \cdot \text{Log}[\text{H}_2\text{SO}_4]_{\text{free}} - b \quad (1)$$

Where a and b are coefficients which depend on temperature and the presence of other metal sulphates. This linear model has been experimentally confirmed and modeled (Figure 5) (Papangelakis et al., 1994). Investigations on the hydrolysis of iron sulphate solution by the same authors highlighted the same linear relationship between the ferric ion and free acid concentrations, but up to a certain point. The solid phase equilibrium curve is actually made of two straight lines of different slopes (Figure 6.). At lower free acidity, the curve describes the hematite equilibrium, and at higher acidity, the curve describes the BFS equilibrium.

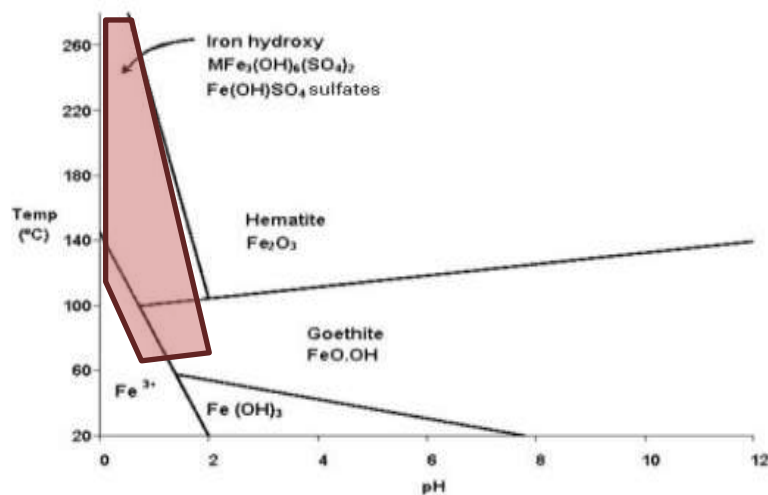


Figure 4 –Areas of stability of the various compounds in the Fe-S-O system (modified after Babcan (1971))

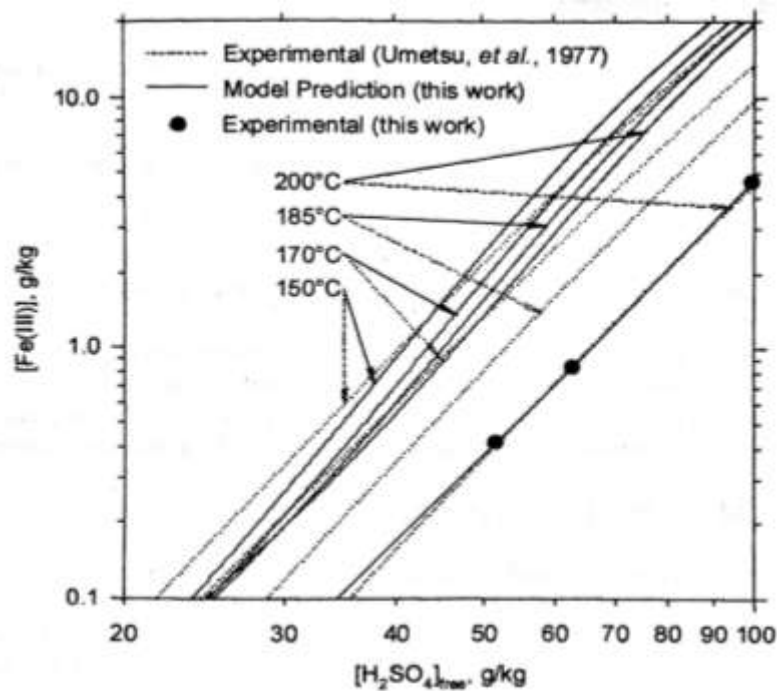


Figure 5 –Hematite solubility – A comparison between model predictions and the experimental data (Papangelakis et al., 1994)

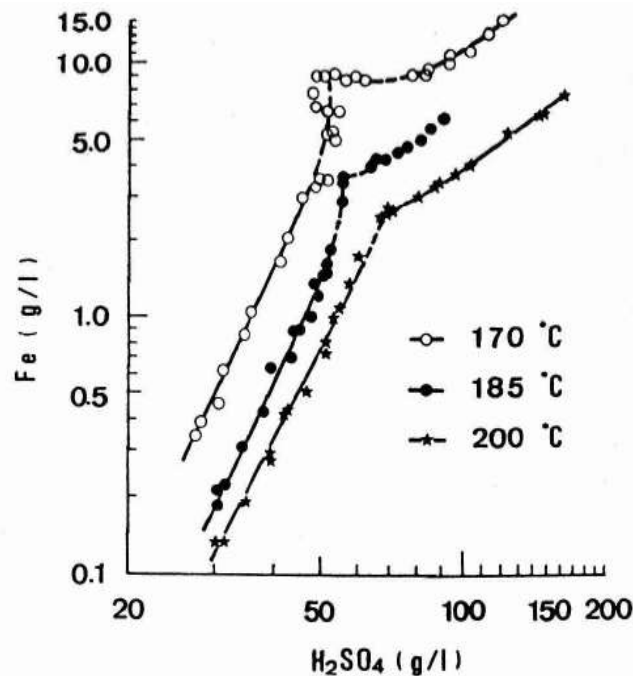


Figure 6 –Relationship between the concentrations of ferric ion and free sulfuric acid in the absence of other metal sulphates (Tozawa & Sasaki, 1986)

Sulphide ores contain many different metals which can be leached along with iron. Common sulphates in leaching solutions are CuSO_4 , ZnSO_4 and Na_2SO_4 . Therefore, assessing their impact on hematite or BFS precipitation is important. Figure 7 shows that the hydrolysis of ferric iron is favored at high temperature and low pH (Umetsu et al., 1977). It can also be seen that for some conditions, only iron precipitates and the other ions stay in solution. Hydrolysis is thus a very efficient way to selectively remove iron from solution.

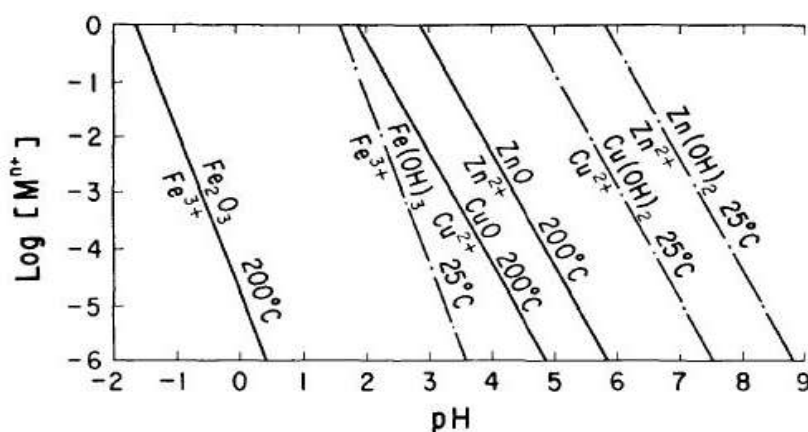
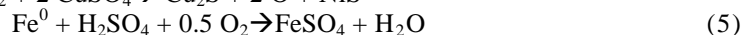
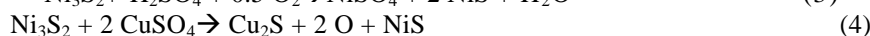
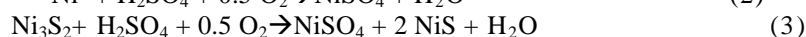
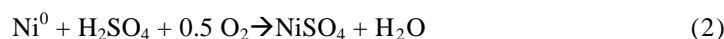


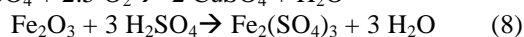
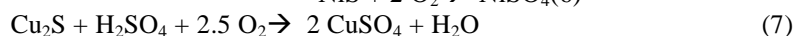
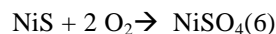
Figure 7 –Relationship between metal ion concentrations and pH at 25°C and 200°C (Umetsu et al., 1977)

V. OPTIMIZATION OF AN INDUSTRIAL HYDROMETALLURGICAL JAROSITE CIRCUIT

An applied study was undertaken to optimize the performance of the Stillwater Base Metals Refinery jarosite precipitation circuit. The goal was to find the multivariate operating parameters to substantially reduce residual iron in solution, consistently to below 10 ppm. The Stillwater Base Metals Refinery (BMR) process consists of matte grinding, atmospheric leaching, pressure leaching, PGM concentrate separation and iron precipitation (Newman & Makwana, 1997). First, the converter matte from the smelter is ground batch-wise in a tower mill to yield a 70 wt.% solids slurry in water, with 80% of the solids passing 74 microns. The ground matte is leached with the recycled acidic pressure leach solution and oxygen in a series of five cascading agitated tanks. Some of the nickel and iron are extracted from the matte, while some of the copper present in the pressure leach solution is precipitated according to the following typical reactions:

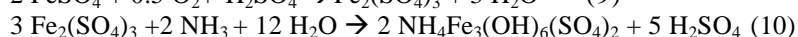
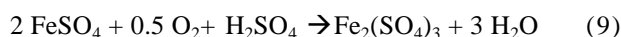


The dissolved iron remains essentially in the ferrous state under the prevailing low pH (2.0 to 2.2) conditions of the atmospheric leach process. Any PGMs present in the feed solution are also co-precipitated with the copper. The residue from the atmospheric leach process is separated by thickening and is then leached further at elevated temperature and oxygen pressure. The atmospheric leach residue consists essentially of millerite (NiS), digenite ($\text{Cu}_{1.8}\text{S}$), djurleite ($\text{Cu}_{1.96}\text{S}$); iron is in the form of magnetite and hydrated ferric oxide. The principal reactions in the pressure leach process are of the type shown below.



Magnetite, if present, does not dissolve at the relatively low acid concentrations (20 to 25 g/L) and temperatures (130 to 135°C) prevailing in the pressure leach process.

The atmospheric leach thickener overflow solution is polish-filtered and then treated to precipitate most of the iron as ammonium jarosite, which is filtered and returned to the smelter. The iron precipitation process is necessary to meet the requirements of the nickel-copper sulphate solution customer. The iron precipitation process also acts as a backstop to precipitate or catch any soluble and insoluble PGMs that may be present in the atmospheric leach solution. The iron is precipitated as ammonium jarosite according to the following reactions.



The plant produces a final readily refined bullion concentrate of about 60% PGM content. As well, by-product nickel sulphate and copper cathode metal are now produced from this zero discharge hydrometallurgical facility.

To carry out this study, bulk representative samples of BMR plant process solutions were provided for laboratory testing. Then, the pertinent controllable plant variables of pH, temperature and reaction time were tested using STAT EASE Design of Experimentation methodology. Because of client budget constraints and time, STAT-EASE statistical software was used to minimize the number of experiments required to identify a statistical representative experimental set. This commercially licensed program based on the fundamentals of design of experiments provides highly efficient:

1. Two-level factorial screening studies so that the vital factors which affect process can be identified
2. Response surface methods to find ideal process settings and achieve optimal performance
3. Mixture design techniques to discover optimal formulations

A complete discourse on the computer software and statistical design of experimentation fundamentals for chemical processing is beyond the scope of this paper, but pertinent references are provided for the reader's convenience (Anderson & Whitcomb 2000; Box & Draper 1987; Box 2000; Cochran 1957; Cornell 1990; Hinkelmann & Kempthorne 1994; Kempthorne 1975; Lorenzen and Anderson 1993; Meyer and Napier-Munn 1999; Montgomery 2001; Napier-Munn and Meyer 1999; Neter 1990; Pazman 1986; STAT EASE 2002; Wu and Hamada 2000; Wayne, Shari, Pat and Mark. 2009). The full factorial design matrix used for this study is illustrated in Table 5.

The results of testing were modeled with an adjusted R-squared fit value of 0.9929 or, in real terms, near perfection. The resultant values and those predicated by the fitted model are shown in Table 6. Below equation 11 illustrates the final statistical model equation in terms of actual plant factors.

$$\frac{1}{(\text{Solution [Fe]})} = -5456.14 + 1861.19 * \text{pH} + 24.54 * \text{T} + 22.11 * \text{t} - 8.35 * \text{pH} * \text{T} - 4.92 * \text{pH} * \text{t} - 0.038 * \text{T} * \text{t} \quad (11)$$

(With concentration [Fe] in g/L, temperature T in F, time t in hrs)

Table 5 – STAT EASE full design matrix for jarosite precipitation optimization

Std	Run	pH	Temp, F	Time, Hrs
4	1	3.5	210	4
7	2	2.9	210	8
6	3	3.5	170	8
2	4	3.5	170	4
1	5	2.9	170	4
3	6	2.9	210	4
8	7	3.5	210	8
5	8	2.9	170	8

Table 6– STAT EASE model fit of jarosite precipitation optimization diagnostic case statistics

Standard Order	Actual Value	Predicted Value	Residual	Leverage
1	3.65	0.42	3.23	0.875
2	250.00	253.23	-3.23	0.875
3	3.73	6.96	-3.23	0.875
4	62.50	59.27	3.23	0.875
5	2.55	5.78	-3.23	0.875
6	250.00	246.77	3.23	0.875
7	9.43	6.21	3.23	0.875
8	43.48	46.71	-3.23	0.875

Figure 8 is a graphical illustration with time held constant at four hours of the results for the iron concentration as a function of temperature and the pH. In essence, the testing and STAT EASE modeling indicated that plant iron concentrations consistently below 10 ppm would be achieved by increasing the pH to 3.5 and lowering the operating temperature to 77°C while keeping the plant residence time the same. In retrospect, this is consistent with the use of ammonia based hydrometallurgical systems. These recommendations were made, implemented in the plant and proved successful.

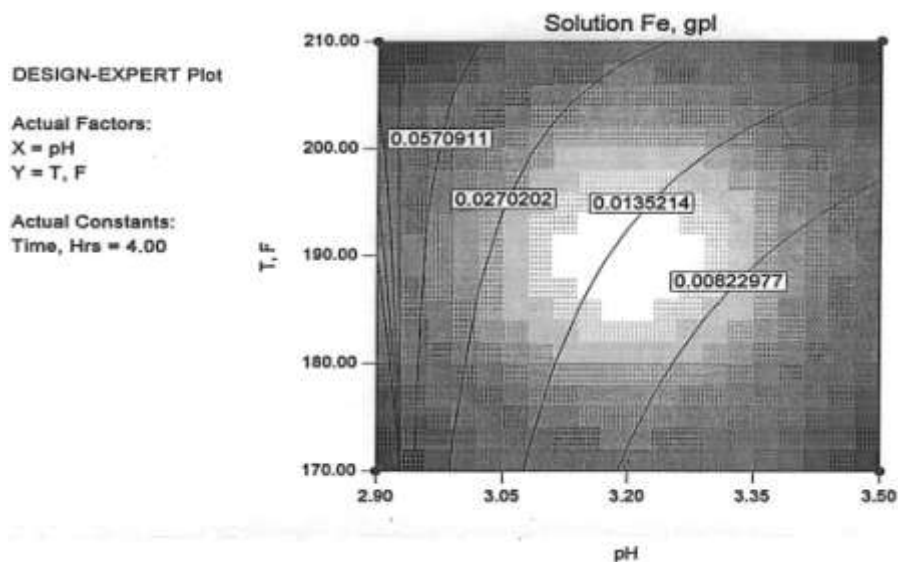


Figure 8 – Graphical illustration of the residual iron concentration at constant time as a function of temperature and pH

VI. SUMMARY

This paper has outlined the fundamental aspects of hydrometallurgical iron precipitation. Then, these principles, coupled with statistical design of experimentation, were successfully applied to optimize iron removal as ammonium jarosite an operating industrial hydrometallurgical facility.

ACKNOWLEDGEMENT

This paper was first published in the proceedings of the XXVIII International Mineral Processing Congress ISBN: 978-1-926872-29-2. Copyright of International Mineral Processing Congress papers will be held by the authors and not the organizing society/body.

REFERENCES

- [1]. Anderson, C.G. and Fayram, T.S. (2013). The use of design of experimentation software in applied flotation testing. *Journal of Powder Metallurgy and Mining*.
- [2]. Anderson, M.J. & Whitcomb, P.J., (2000) *DOE Simplified: Practical Tools for Effective Experimentation*, ISBN: J-56327-225-3, Productivity, Inc.
- [3]. Babcan, J., (1971). Synthesis of jarosite $KFe_3(SO_4)_2(OH)_6$. *Geol. Zb*, 22(2), 299-304.
- [4]. Bigham, J.M. & Nordstrom, D.K. (2000). Iron and aluminum hydroxysulphates from acid sulphate waters. *Reviews in Mineralogy and Geochemistry*, 40(1), 351-403.
- [5]. Box, G.E.P., & Draper, N.R., (1987). *Empirical Model Building and Response Surfaces* ISBN: 0-471-81033-9, Wiley-Interscience.
- [6]. Box, G.E.P., (2000). *Box on Quality and Discovery: with Design, Control, and Robustness*, Wiley, New York.
- [7]. Burgina, E.B., Kustova, G.N., Nikitenko, S.G., Kochubei, D.I., & Elizarova, G.L. (1996). Comparative study of the structures of some basic iron (III) sulphates. *Journal of Structural Chemistry*, 37(2), 240-246.
- [8]. Cheng, T.C. & Demopoulos, G.P. (2004). Hydrolysis of ferric sulphate in the presence of zinc sulphate at 200 C: precipitation kinetics and product characterization. *Industrial & engineering chemistry research*, 43(20), 6299-6308.
- [9]. Cochran, W.G., (1957). *Experimental Designs*, Wiley, New York.
- [10]. Cornell, J., (1990). *Experiments with Mixtures: Designs, Models, and the Analysis of Mixture Data*, 2nd Ed., ISBN: 0-471-52221-X, John Wiley and Sons.
- [11]. Dutrizac, J.E. & Jambor, J.L., (2000). Jarosites and their application in hydrometallurgy. *Reviews in Mineralogy and Geochemistry*, 40(1), 405-452.
- [12]. Dutrizac, J.E., & Chen, T.T., (2012). Behavior of various impurities during the precipitation of hematite from ferric sulphate solutions at 225° C. In *TT Chen Honorary Symposium on Hydrometallurgy, Electrometallurgy and Materials Characterization*, (pp. 489-507). John Wiley & Sons, Inc.
- [13]. Fleming, C.A., (2010). Basic iron sulphate—a potential killer in the processing of refractory gold concentrates by pressure oxidation. *Minerals & Metallurgical Processing Journal*, 27(2), 81-88.
- [14]. Fleuriault, C.M. (2016). Iron phase control during pressure leaching at elevated temperature, MSc Thesis, Kroll Institute for Extractive Metallurgy, Colorado School of Mines, Golden, Colorado
- [15]. Fleuriault, C.M., Anderson, C. G. & Shuey, S. (2016) Iron phase control during pressure leaching at elevated temperature, Manuscript in publication.
- [16]. Gathje, J.C., (2006). Iron reduction in copper leach liquors using controlled precipitation of sulphate species during high temperature pressure oxidation of base metal ores. *Iron Control Technologies*, CIM, Montreal, 2006, 231-246.

- [17]. Gupta, C.K., and Mukherjee, T.K., (1990). Hydrometallurgy in Extraction Processes. Vol. 2. CRC Press, 196-200.
- [18]. Habashi, F., (1999). Textbook of Hydrometallurgy. Métallurgie Extractive Québec.
- [19]. Hinkelmann, K. & Kempthorne, O., (Editors), (1994). Design and Analysis of Experiments: Introduction to Experimental Design, ISBN: 0471551783, John Wiley & Sons.
- [20]. Kempthorne, O., (1975). The Design and Analysis of Experiments, Published 1975, Robert E. Krieger Publishing Co., Huntington, New York.
- [21]. Lazaroff, N., Sigal, W., & Wasserman, A., (1982). Iron oxidation and precipitation of ferric hydroxysulphates by resting *Thiobacillus ferrooxidans* cells. Applied and Environmental Microbiology, 43(4), 924-938.
- [22]. Lorenzen, T.J. and Anderson, V.L., (1993). Design of Experiments: A No-Name Approach, ISBN: 0-8247-9077-4, M. Dekker, New York.
- [23]. Meyer D. & Napier-Munn T.J., (1999). Optimal Experiments for Time Dependent Mineral Processes, Australian and New Zealand Journal of Statistics.
- [24]. Mohemius, A. 2016, The Iron Elephant: A Brief History of Hydrometallurgists Struggle With Element 26, 13 pgs. Iron Control Practice and Research, Proceedings of the 46th Annual Hydrometallurgy Meeting, CIM, Quebec City, Quebec, Canada
- [25]. Montgomery, D.C, (2001). Design and Analysis of Experiments, 5th Ed., ISBN: 0-471-31649-0, John Wiley and Sons.
- [26]. Napier-Munn T.J. & Meyer D.H., (1999). A modified paired T-test for the analysis of plant trials with auto correlated in time, Minerals Engineering, 12(9), 1093-1109.
- [27]. Neter, J., (1990). Applied Linear Statistical Models: Regression, Analysis of Variance, and Experimental Designs, Irwin, Homewood, Illinois.
- [28]. Newman, L. and Makwana, M., (1997). Commissioning of the Stillwater Mining Company Base Metals Refinery, Hydrometallurgy and Refining of Nickel and Cobalt, Proceedings of the 27th Annual Hydrometallurgical Meeting, The Metallurgical Society of CIM, Sudbury, Ontario, Canada.
- [29]. Papangelakis, V.G., Blakey, B.C., & Liao, H. (1994). Hematite solubility in sulphate process solutions. In Hydrometallurgy'94 (pp. 159-175). Springer, The Netherlands.
- [30]. Pazman, A. (1986). Foundations of Optimum Experimental Design, D. Reidel, Boston.
- [31]. Posnjak, E., & Merwin, H.E. (1922). The system $\text{Fe}_2\text{O}_3\text{-SO}_3\text{-H}_2\text{O}$. Journal of the American Chemical Society, 44(9), 1965-1994.
- [32]. Rossman, G.R. (1976). Spectroscopic and magnetic studies of ferric iron hydroxy sulphates: the series $\text{Fe}(\text{OH})\text{SO}_4 \cdot n\text{H}_2\text{O}$ and the jarosites. American Mineralogist, 61(5-6), 398-404.
- [33]. Scordari, F. (1981). Fibroferrite: A mineral with a $\{\text{Fe}(\text{OH})(\text{H}_2\text{O})_2\text{SO}_4\}$ spiral chain and its relationship to $\text{Fe}(\text{OH})\text{SO}_4$, butlerite and parabutlerite. Tschermaks mineralogische und petrographische Mitteilungen, 28(1), 17-29.
- [34]. STAT-EASE (2002). Design-Expert Reference Manual, STAT-EASE Corporation, Minneapolis, Minnesota, 2002.
- [35]. Tourre, J-M. (1984). A study of the conditions of formation of silver-containing jarosites in the acid pressure leaching of pyritic ores. PhD Diss. Colorado School of Mines.
- [36]. Tozawa, K., & Sasaki, K. (1986). Effect of coexisting sulphates on precipitation of ferric oxide from ferric sulphate solutions at elevated temperatures. Iron Control in Hydrometallurgy, Ellis Horwood, Chichester, England, 454-476.
- [37]. Turk, D.J., (2000). Stillwater Mining Company Nye Concentrator Operation, SME Annual Meeting, Preprint 00-10, Salt Lake City, Utah, February.
- [38]. Umetsu, V., Tozawa, K., & Sasaki, K.I. (1977). The hydrolysis of ferric sulphate solutions at elevated temperatures. Canadian Metallurgical Quarterly, 16(1), 111-117.
- [39]. Van Santen, R.A. (1984). The Ostwald step rule. The Journal of Physical Chemistry, 88(24), 5768-5769.
- [40]. Voigt, B., & Göbler, A. (1986). Formation of pure haematite by hydrolysis of iron (III) salt solutions under hydrothermal conditions. Crystal Research and Technology, 21(9), 1177-1183.
- [41]. Wayne, Shari, Pat and Mark". (2009). Handbook for Experimenters. Stat-Ease 08.1.
- [42]. Wu, C.J.F. & Hamada, M. (2000). Experiments: Planning, Analysis, and Parameter Design Optimization, ISBN: 0-471-25511-4, Wiley.

*Dr. Corby G. Anderson. "The Optimization of An Industrial Ammonium Production Circuit." American Journal of Engineering Research (AJER), vol. 06, no. 12, 2017, pp. 119-128.